Hole transport in polyfluorene-based sandwich-type devices: Quantitative analysis of the role of energetic disorder

S. L. M. van Mensfoort,[1,2,][*] S. I. E. Vulto,[2] R. A. J. Janssen,[1] and R. Coehoorn[1,2]

[1]*Molecular Materials and Nanosystems, Department of Applied Physics, Eindhoven University of Technology, P.O. Box 513, 5600 MB Eindhoven, The Netherlands*
[2]*Philips Research Laboratories, Professor Holstlaan 4, 5656 AE, Eindhoven, The Netherlands*

The current density versus voltage $[J(V)]$ curves of hole-only sandwich-type devices containing a blue-emitting polyfluorene-based copolymer were measured for a wide range of temperatures and for several thicknesses of the active organic layer. We show that the $J(V)$ curves cannot be accurately described using a commonly used model within which the mobility depends only on the electric field, but that a consistent and quantitatively precise description of all curves can be obtained using the recently introduced extended Gaussian disorder model (EGDM). Within the EGDM, the mobility depends on the electric field *and* on the carrier concentration. Two physically interpretable parameters, viz. the width of the density of states, σ, and the density of transport sites, N_t, determine the shape of the curves. For the semiconductor studied, we find $\sigma = 0.13 \pm 0.01$ eV and $N_t = (6 \pm 1) \times 10^{26}$ m^{-3}. Consistent with the EGDM, the logarithm of the mobility in the low carrier concentration and low-field limit is found to show a $1/T^2$ temperature dependence. It is shown that analyses which neglect the carrier-concentration dependence of the mobility yield an apparent $1/T$ temperature dependence, as reported for many different materials, and that the incorrectness of such an approach would readily follow from a study of the layer thickness dependence of the mobility.

PACS number(s): 73.40.Sx, 72.20.Ee, 85.30.De

I. INTRODUCTION

The efficiency of organic light-emitting diodes (OLEDs), which are currently being developed for display[1,2] and lighting[3] applications depends crucially on the electron and hole mobilities. In single-layer OLEDs with ideally injecting contacts, e.g., the ratio between the electron and hole mobilities determines the shape of the recombination profile,[4] and thereby the outcoupling efficiency.[5] Furthermore, the shape of the recombination profile is determined by the detailed functional dependence of the mobility on the electric field, the charge carrier concentration, and the temperature. Similarly, in the case of multilayer OLEDs, with a central emissive layer that can consist of sublayers with different emission colors, the electron and hole mobilities in the central layer determine the recombination profile,[6] and thereby the emission color.

At present, a lack of consensus on the proper physical description of the hopping mobility in realistic OLED systems hampers progress toward a quantitative model with predictive value for the current density and luminance as a function of the voltage. On the one hand, it has been proposed that the mobility is determined by the activation energy for polaron hopping between essentially equivalent "transport sites," which may be associated with single molecules or (in a polymer) with conjugated segments.[7] A distinct signature of this hopping process would be the observation of a $1/T$ dependence of the logarithm of the mobility, μ. On the other hand, it has been argued that the mobility in actual organic semiconductors is predominantly determined by the energetic disorder of the transport sites. For the case of a Gaussian density of states (DOS), Bässler and coworkers found from Monte Carlo calculations that within this Gaussian disorder model (GDM) the logarithm of the mobility at small

carrier concentrations, for which the carriers act as independent particles (Boltzmann limit), varies as $1/T^2$.[8,9] Studies of the temperature dependence of the hole mobility in organic electronic materials, e.g., from time-of-flight measurements,[10] dark-injection transients[11] or from steady-state current-voltage $[J(V)]$ measurements[12,13] have provided support for both types of models.[12] Additionally, an increase in the mobility is often found from experiments with increasing bias voltage. Conventionally, this is attributed to an exponential electric-field dependence of the mobility, as given by the so-called Poole-Frenkel factor (see Eq. (1) in Sec. III A).[8,12,14–18]

From work on inorganic semiconductors it has already been known for a long time that disorder not only affects the temperature and field dependence of the mobility, but also leads to a carrier-concentration dependence (see Ref. 19 and references therein). For transport in organic semiconductors, this effect has been demonstrated first by Vissenberg and Matters who studied organic field-effect transistors.[20] The mobility was analyzed assuming transport in an exponential DOS. In materials used in OLEDs, the effect also plays an important role, as demonstrated, e.g., by Maennig *et al.*[21] for *p*-doped organic semiconductors used as injection layers. These results were explained assuming an exponential DOS (Ref. 21) or a Gaussian DOS.[22] For undoped sandwich-type diodes, based on the polymer poly(*p*-phenylene vinylene) (PPV, frequently used in OLEDs), the importance of the effect was first demonstrated by Tanase *et al.*[23] At a sufficiently small carrier concentration the mobility was found to be constant, and above a certain cross-over concentration the mobility was found to increase with increasing concentration.

These experimental findings for PPV can be well explained using the extended Gaussian disorder model (EGDM) introduced by Pasveer *et al.*[24] (see also Ref. 25 and

references therein). It follows from the EGDM that such a transition is expected for carrier concentrations above the concentration beyond which the carriers can no longer be considered as independent particles. In contrast, polaron models do not predict a carrier-concentration dependence of the mobility.[26] A drift-diffusion device model which includes the carrier-concentration dependence of the mobility in a Gaussian DOS was first presented by Roichman *et al.*[27] Recently, an extensive modeling study of the consequences of Gaussian disorder on the $J(V)$ curves was carried out by Van Mensfoort and Coehoorn.[28] The authors showed that, if in the analysis the carrier density dependence of the mobility is (incorrectly) neglected, the resulting *apparent* mobilities are strongly layer thickness dependent. A similar conclusion was given by Craciun *et al.*[29] from an analysis of experimental $J(V)$ curves for a series of hole-only devices with different thicknesses, based on poly(2-methoxy,5-(2′-ethyl-hexoxy)-*p*-phenylene vinylene) (MEH-PPV), using a more phenomenological mobility model. In spite of this progress, it is presently not well established (i) to what extent the mobility as predicted within the EGDM can consistently describe the $J(V)$ curves of commonly used organic semiconductors, (ii) how extended the experimental set of available steady-state $J(V)$ curves should be in order to be able to discriminate between the EGDM and a "conventional" mobility model that neglects the carrier-concentration dependence of the mobility and assumes a Poole-Frenkel field dependence of the mobility, and (iii) why commonly used methods for analyzing the experimental data often lead to a $1/T$ temperature dependence of the mobility, even when there is clear evidence of the predominant role of disorder.

The purpose of this paper is to address these three issues by performing a detailed quantitative analysis of the temperature, layer thickness, and voltage dependence of the current density for sandwich-type hole-only devices containing a polyfluorene (PF)-based organic semiconductor. PF-based polymers are a promising candidate for application in blue polymer LEDs and are a widely studied class of polymers.[11,14,30,31] The materials studied in this paper have been used in the 13″ full-color OLED-TV display demonstrated by Philips in 2005.[32] Also, blue-emitting organic materials are key as a matrix material in most common white OLEDs. First, it is shown that the EGDM provides a fully consistent description of all experimental data, whereas an analysis of the data using a "conventional" approach with a carrier-concentration-independent mobility with a field dependence as described by a Poole-Frenkel factor cannot consistently explain all data. Second, we show that a variation of the device thickness is necessary to distinguish between the conventional mobility model and a carrier-concentration-dependent mobility model, in agreement with the conclusions presented by Blom *et al.* for PPV-based hole-only devices.[33]

In order to arrive at these two conclusions, we have extended previous analyses of the validity of various mobility models in several directions. In a preliminary study, we have analyzed the hole mobility in the PF polymers using only the conventional model,[34] and neglecting charge carrier diffusion. In the work by Pasveer *et al.*[24] on PPV-based devices,

an analysis of $J(V)$ curves PPV-based hole-only devices within the EGDM was carried out, but also neglecting diffusion. Furthermore, that study was limited to only one layer thickness. In the work of Blom and coworkers on PPV-based hole-only devices[29,33] the quantitative analyses were limited to room-temperature measurements, and the $J(V)$ curves were not analyzed using the EGDM but, instead, by a more phenomenological approach. In our present analysis, we do not only consider the layer thickness *and* temperature dependence of the $J(V)$ curves, but we also include, for the first time, a comparison with the predictions based on the EGDM *and* a conventional model for the mobility. Furthermore, all analyses given here are carried out using a drift-diffusion device model.[28] Thereby, we have been able to significantly extend the voltage range used for critically analyzing the validity of both models, to values well below the built-in voltage, V_{bi}.

The third issue, on the $1/T$ versus $1/T^2$ paradox in the temperature dependence of the mobility, is addressed by re-analyzing the measured $J(V)$ curves using an approach that is often employed for quickly deducing the mobility from the raw data. Recently, Craciun *et al.*[35] applied such an (over-simplified) analysis to a large number of disordered organic semiconductors and showed (i) that this leads to a $1/T$ dependence of the effective low-field mobility, (ii) that the effective mobility at each given temperature depends on the device thickness, and (iii) that in the infinite temperature limit the mobility extrapolates to a single value which is independent of the thickness (and even of the material). The authors suggested that these findings can be explained from the EGDM. An analysis of our data, carried out similarly as in Ref. [35], indeed reveals a $1/T$ dependence of the effective mobility for the temperature range studied. Furthermore, we predict from the EGDM that the effective mobility is indeed strongly thickness dependent, even up to very large thicknesses. However, in contrast to the findings reported by Craciun *et al.*, we show that within the EGDM the $\log[\mu(1/T)]$ curves for different thicknesses do not extrapolate to a single value for $1/T \rightarrow 0$, but instead are tangents to a parabolic $\log(\mu_0) \propto 1/T^2$ curve, where μ_0 is the low-field mobility in the low-carrier density (Boltzmann) limit. The effective $1/T$ dependence is shown to be the result of the carrier-concentration dependence of the mobility, as suggested already by Coehoorn *et al.*[25]

In Sec. II the sample preparation and measurement techniques are outlined, and the measured $J(V)$ curves are presented. Section III discusses the analysis of these results using the conventional mobility model and using the EGDM. The method to determine the optimal model parameters is outlined. In Sec. IV, the origin of the apparent $1/T$ dependence of the mobility is discussed. Section V contains a summary and conclusions.

II. EXPERIMENTAL RESULTS

For fabricating the sandwich-type hole-only devices studied, a hole-conducting layer of poly(3,4-ethylenedioxythiophene):poly(styrenesulphonic acid) (PEDOT:PSS) (Ref. [36]) of 100 nm is deposited under clean room condi-
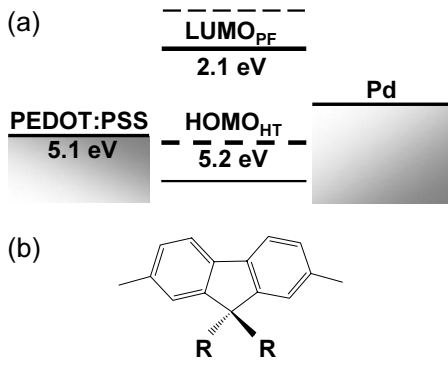
FIG. 1. (a) Schematic representation of the energy levels in the devices studied, indicating the HOMO and LUMO levels of the HT units of the polymer (dashed) and of the PF units (solid), and the Fermi levels of the PEDOT:PSS and the palladium electrode. All energies are given with respect to the vacuum level. (b) Schematic chemical structure of the fluorene monomer units, which are copolymerized with HT units in order to form the light-emitting polymer used.

tions by spincoating on precleaned glass substrates patterned with indium tin oxide (ITO). After drying, the PEDOT:PSS-coated substrate is annealed at 200 °C for 10 min to evaporate the solvent (water). Subsequently, the polyfluorene-based light-emitting polymer (LEP) layer is deposited by spincoating from a toluene solution in a nitrogen glovebox, resulting in LEP layer thicknesses L in the range 60–125 nm. The LEP layer thicknesses were determined from step-height measurements using a Veeco™ Dektak stylus profilometer. In a high-vacuum environment palladium is evaporated through a mask to form ∼100 nm-thick top electrodes. The total sample structure is thus (glass|ITO|PEDOT:PSS|LEP|Pd). To protect the devices from water and oxygen contamination, the devices are encapsulated using a metal lid enclosing a desiccant getter. For each LEP layer thickness 27 nominally identical 3 × 3 mm^2 devices were prepared on a single substrate.

The LEP is a blue-emitting polymer, from the Lumation™ Blue Series, supplied by Sumation Co., Ltd. The polymer consists mainly of fluorene units, with copolymerized hole transport (HT) units that facilitate injection of holes from the anode. The energy levels of the highest occupied molecular orbitals (HOMOs) and lowest unoccupied molecular orbitals (LUMOs) of the PF and HT units, and the chemical structure of the PF units are schematically shown in Fig. 1.[34] From cyclic voltammetry (CV) and x-ray photoemission spectroscopy (XPS) measurements, the polyfluorene HOMO energy is known to be 5.8 eV, leading to a large injection barrier from the PEDOT:PSS electrode.[34] The hole transport takes place via the HT units, for which the HOMO energy (5.2 eV from CV measurements[34]) is well separated from that of polyfluorene. In contrast to polymers like PPV derivatives, where holes are delocalized over several chain segments, the holes on the PF-based copolymer used are localized on the HT units, which are present in a concentration well above the threshold which ensures "guest-to-guest" transport.[15] As all available transport models are based on the assumption of hopping between *localized* sites, the semiconductor studied
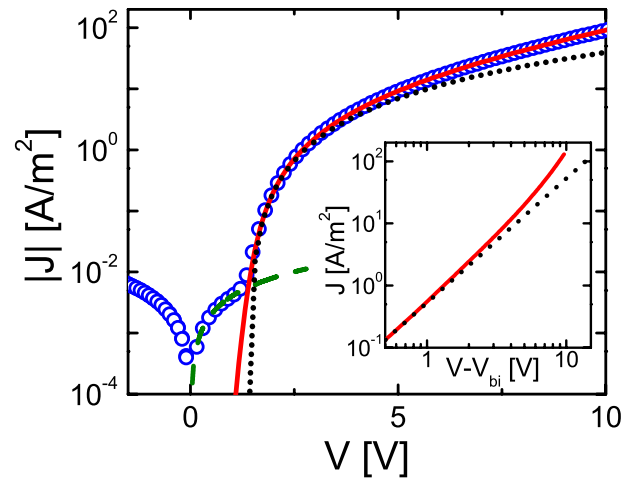

FIG. 2. (Color online) Measured $J(V)$ curve for $L=122$ nm at $T=295$ K (open circles). The symmetric part of the curve around $V=0$ V is fitted linearly (dashed) and subtraction of this leakage current results in the corrected $J(V)$ curve (full). The dotted curve gives a fit using the Mott-Gurney formula [Eq. (2)], with $V_{bi} =1.38$ V (here). The inset shows the corrected experimental $J(V)$ curve and the Mott-Gurney fit on a log-log scale (see Sec. IV).

is a very suitable model material for comparing the suitability of various transport models. In a double carrier device based on this polymer, the electron transport takes place via the LUMO of the PF units, at 2.1 eV.[34] The devices with Pd electrodes, used in this study, were found to properly function as single carrier devices. No light emission was detected up to the highest voltages used, indicating the presence of a sufficiently large electron injection barrier at the cathode. Analyses of the $J(V)$ curves yield a built-in voltage, V_{bi}, of approximately 1.9 V (see Sec. III B), which would yield an effective Fermi energy of ∼3.2 eV for the Pd cathode. This is much smaller than as expected from its vacuum work function (∼5.1 eV). Similar differences between the vacuum work function and the effective work function of metal electrodes in organic devices have been observed in many other studies.[37]

Current-voltage measurements as a function of temperature are performed using a LabView controlled Keithley 2400 SourceMeter. The temperature is controlled by a feedback system, consisting of a cooled nitrogen flow, a heater, a Thermocoax 2AB25 thermocouple (type K) on the substrate and an Oxford Intelligent Temperature Controller ITC4. The temperature is kept constant during each measurement and is set per measurement in the range −120 to +20 °C. Four-point impedance spectroscopy measurements were performed using a Schlumberger SI-1260 Impedance/Gain-Phase Analyzer to determine the capacitance of the diodes at low frequencies. From the geometrical capacitance, typically measured at small negative and small positive voltages, the dielectric constant, ε_r, of the polymer in thin film was determined using the thicknesses from the step-height measurements, leading to $\varepsilon_r=3.2\pm0.1$.

Figure 2 shows the $J(V)$ curve of a hole-only diode with a thickness of 122 nm measured at room temperature (open circles). The results of all 27 devices of this thickness on one
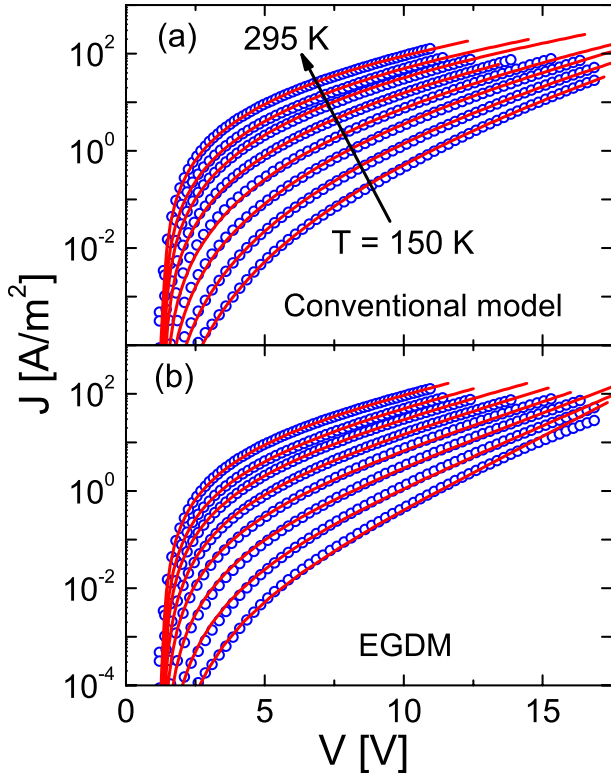
FIG. 3. (Color online) $J(V)$ curves after leakage current correction (see text) for a device with $L=122$ nm, at $T=150$, 171, 193, 213, 233, 253, 271 and 295 K (open circles). The solid lines are the result of drift-diffusion simulations using (a) the conventional mobility model [Eq. (1)] and (b) the extended Gaussian disorder model [Eqs. (3)–(5)]. The full curves shown in Fig. 3(b) were obtained using $N_t=6\times10^{26}$ m^{-3} and $\sigma=0.13$ eV. The (remaining) model parameters used in Figs. 3(a) and 3(b) are discussed in the text.

substrate are almost identical, with variations smaller than a factor of 2 in the current. For small voltages, the current density is symmetric around $V=0$ V and shows a linear voltage dependence (Ohmic). This current is commonly attributed to either (i) leakage paths through the organic layer, (ii) leakage paths inherent to the sample structure, (iii) intrinsic conduction due to impurities in the organic layer, or to (iv) minority carrier injection,[38] and is commonly called a "leakage current." We corrected the measured $J(V)$ curve for the extrapolated leakage current obtained by a linear fit to the current in the low-voltage regime (dashed line). The resulting $J(V)$ curves (solid line) are used for further analysis. Figure 3 shows the corrected $J(V)$ curves (open circles) for the same device for temperatures in the range 150–295 K, in steps of approximately 20 K.

III. ANALYSIS OF $J(V)$ CURVES

A. Analysis assuming the conventional mobility model

Within conventional mobility models (see, e.g., Refs. 7(c), 8, 12, 14–18, and 39), the mobility is assumed to be field dependent as described by

$$\mu(F(x),T) = \mu_0(T)\exp[\gamma(T)\sqrt{F(x)}]. \qquad (1)$$

Here μ_0 is the mobility at field $F=0$, and x is the position within the LEP layer. In the exponential Poole-Frenkel factor, the temperature-dependent parameter γ determines the field dependence. Within the simplest possible approach, the field dependence of the mobility is neglected, only the drift contribution to the current density is taken into account (no diffusion), and the contacts are assumed to be ideal (infinite carrier density at the injecting interface). The relation between the current density and the voltage in a single carrier device is then given by the Mott-Gurney (MG) square law[40]

$$J = \frac{9}{8}\varepsilon_0\varepsilon_r\mu\frac{(V-V_{bi})^2}{L^3}, \qquad (2)$$

for $V>V_{bi}$, with ε_0 as the vacuum permittivity. The dotted curve in Fig. 2 shows the result of an analysis using this expression, with $V_{bi}=1.38$ V (here), which gives rise to an optimal fit for intermediate voltages (around 2 V). Below 1.4 V and above 2.5 V the experimental $J(V)$ curve deviates significantly from the MG relation.

The quality of the fit is improved by including diffusion, which gives rise to an important additional current density at voltages below and around V_{bi}, and by making use of Eq. (1), which provides a better description of the data at high voltages. Analyses of $J(V)$ curves using the MG relation often involve the choice of an empirical value of V_{bi}, in order to obtain a good fit at $V>V_{bi}$. When properly taking diffusion into account, such an approach is no longer necessary, as the full $J(V)$ curve can be simulated, also for $V<V_{bi}$. This makes it possible to more critically assess the validity of proposed transport models. We incorporated Eq. (1) in a recently developed efficient drift-diffusion model,[28] which simultaneously solves the current continuity equation and the Poisson equation. For each temperature, we determine the values of μ_0 and γ that best fit the experimental data in Fig. 3(a). V_{bi} was taken equal for all temperatures. The hole injection barrier at the anode is assumed to be small (≤ 0.1 eV, see Fig. 1) and is believed not to limit hole injection. The calculations are performed using a hole density at the anode $p(0)$ equal to 1.8×10^{26} m^{-3}, which is equal to the estimated density of hole transporting units in the polymer.[34] We find that a change of $p(0)$ over approximately one order of magnitude does not significantly change the $J(V)$ results. The carrier density at the cathode, $p(L)$, follows then from V_{bi}, using $p(L)=p(0)\exp[-eV_{bi}/(k_BT)]$, with e as the elementary charge and k_B the Boltzmann constant.

The full lines in Fig. 3(a) show the best fits to the experimental curves for the 122 nm devices. We find $V_{bi}=1.62\pm0.05$ V. This value is in excellent agreement with the built-in voltage determined from an analysis of capacitance-voltage experiments on the same samples, assuming the conventional model.[41] Figure 4 shows the temperature dependence of μ_0 and γ. These parameters follow an empirical $1/T$ temperature dependence, as observed for many other organic semiconductors.[12,17,42]

It is clear from the solid curves in Fig. 3(a) that this approach leads to excellent fits *for this single device thickness*. To ultimately test the validity of the conventional model, we
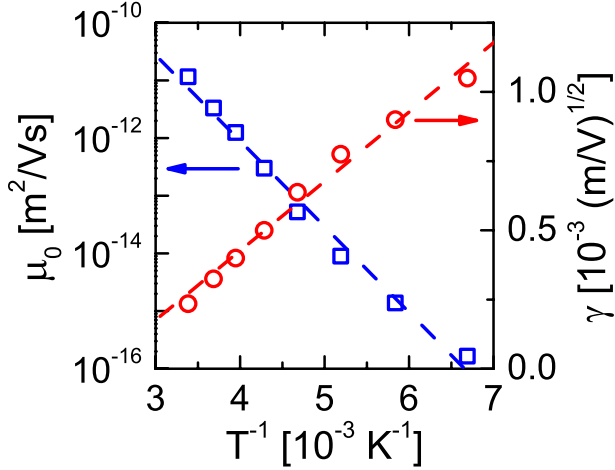
FIG. 4. (Color online) Mobility model parameters μ_0 (squares) and γ (circles) as a function of $1/T$, as determined using the conventional mobility model [Eq. (1)] for the 122 nm devices, for which the $J(V)$ curves are shown in Fig. 3. The dashed lines are empirical $1/T$ fits.

varied the thickness of the active layer. The parameters optimized for the thickest device (122 nm) were used to predict the $J(V)$ outcome for thinner devices. Figures 5(a) and 5(b) show the experimental and modeled $J(V)$ curves, using the conventional mobility model, for $L=122$, 98 and 67 nm at room temperature and at 170 K, respectively. For the 98 and 67 nm devices, the calculated $J(V)$ curves seem to properly describe the measured room-temperature data at low voltages. However, above 2.5 V (7.5 V) for the 67 nm (98 nm) device, the calculations underestimate the current density. At
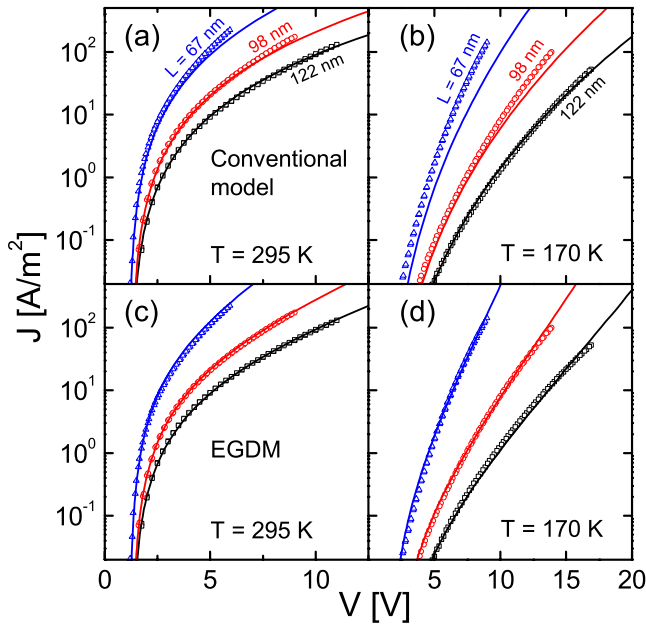
170 K, the deviations are even more pronounced. Already at low voltages the model then fails to describe the $J(V)$ curves of the thinner devices.

It is highly unlikely that the discrepancies between the measurements and the predictions are caused by the manifestation of an injection limitation, instead of being an indication of the failure of the conventional model. The effect of an injection limitation increases with decreasing layer thickness, so that one would then expect that the parameter set which provides the best fit for the thickest device would overestimate the current density for the thinner devices. However, the observed trend is opposite. We therefore conclude that the analysis clearly proves that the conventional model fails to consistently describe the effect of a thickness variation on the $J(V)$ curves.

B. Analysis using the extended Gaussian disorder model

Within the extended Gaussian disorder model, introduced by Pasveer et al.,[24,25] the mobility in disordered organic semiconductors does not only depend on the electric field, but, for realistic disorder parameters, also strongly on the charge carrier density. The mobility depends on the width of the Gaussian density of states, σ, the total volume density of transport sites, N_t, and the decay length of the localized wave functions of the states in between which hopping takes place. As motivated in Ref. 24, we assume that this length is a factor of 10 smaller than the average intersite distance, $a = N_t^{-1/3}$. In Ref. 25, it has been shown that the actual value of the decay length has no effect on the carrier-concentration dependence of the mobility, and has only a limited effect on the shape of the temperature dependence. As shown in Ref. 24, the mobility can be written as

$$\mu(p,F,T) = \mu_{0,\text{EGDM}}(T)f(F,T)\exp\left[\frac{1}{2}(\hat{\sigma}^2 - \hat{\sigma})\left(2\frac{p}{N_t}\right)^\delta\right],$$

(3)

where $\mu_{0,\text{EGDM}}$ is the mobility in the $F=0$ and zero carrier density limit, $\hat{\sigma} = \sigma/(k_BT)$ is the dimensionless disorder parameter, $\delta = 2[\ln(\hat{\sigma}^2 - \hat{\sigma}) - \ln(\ln 4)]/\hat{\sigma}^2$, and where the field dependence of the mobility is given by

$$f(F,T) = \exp\left[0.44(\hat{\sigma}^{3/2} - 2.2)\right]\left[\sqrt{1 + 0.8\left(\frac{eaF}{\sigma}\right)^2} - 1\right].$$

(4)

The carrier concentration and electric-field-dependent diffusion coefficient is given by the generalized Einstein equation[43]

$$D(p,F,T) = \frac{k_BT}{e}\mu(p,F,T)\frac{1}{k_BT}\frac{p}{\left.\frac{dp(E_F)}{dE_F}\right|_p},$$

(5)

where E_F is the Fermi energy. The function $p(E_F)$ follows from the filling of the Gaussian DOS, using Fermi-Dirac statistics. We note that the mobility depends on the position in the device, via the x-dependence of p and F.

For small carrier concentrations, within the so-called Boltzmann regime, the mobility is independent of the carrier

FIG. 5. (Color online) Measured (symbols) and calculated (lines) $J(V)$ curves for $L=122$, 98 and 67 nm at $T=295$ and 170 K. (a–b) Calculations using the conventional mobility model with the parameters optimal for the 122 nm device. (c–d) Calculations using the EGDM, with $\sigma=0.13$ eV and $N_t=6\times10^{26}$ m^{-3}.

density, and there is no enhancement of the diffusion coefficient beyond the value expected from the standard Einstein equation ($D = k_B T \mu / e$). Within this regime, the carriers may be viewed as independent particles. Above a certain crossover concentration, the mobility increases with increasing concentration. The deepest sites in the tail of the Gaussian DOS can then no longer act as effective trap sites, as they are with a high probability already occupied by carriers. A detailed discussion of the mobility in a Gaussian DOS, and of the carrier concentration and field dependence of the mobility and diffusion coefficient as a function of $\sigma / (k_B T)$, is given in Refs. 25 and 28, respectively. In OLEDs based on materials with a realistic degree of disorder ($\sigma / (k_B T) = 4$ to 6 at room temperature) the carrier concentration is in a large part of the device larger than the cross-over concentration $c^* = (1/2) \exp[-\hat{\sigma}^2 / 2]$ [$\sim 10^{-4}$ to 10^{-8} for $\sigma / (k_B T) = 4$ to 6 (Ref. 25)]. As will be demonstrated further below, taking the carrier-concentration dependence of the mobility into account is therefore very important.

At very high carrier concentrations, i.e., when the DOS is close to half-filled, the hopping distance for charge carriers toward an unoccupied and energetically favorable site increases and therefore the mobility starts to decrease for c close to 0.5. The effect of the occupation of final states on the mobility is taken into account in Eqs. (3) and (4), which provide an excellent description of the numerically exact results given in Ref. 24 up to $c \approx 0.1$.[25] An improved agreement with the exact result at higher concentrations was obtained by introducing a cut-off concentration, $c_{\text{cutoff}} = 0.1$, above which the mobility is assumed to be equal to $\mu(c_{\text{cutoff}})$.[28] A second effect which plays a role at high carrier densities is the Coulomb interaction between the carriers. In the numerical calculations of the mobility given in Ref. 24, on which Eqs. (3) and (4) are based, this effect was neglected. The effect of including the Coulomb interaction was addressed by Zhou *et al.*,[44] who showed that it is only significant above $c = 10^{-2}$. The high carrier density interface region near the anode where final-state effects and the Coulomb interaction play a role is very thin and has a high conductance. In order to investigate the sensitivity of the analyses given in this paper to the mobility in this region, we have varied the cut-off concentration. For c_{cutoff} in the range 0.01 to 0.5 no significant effect on the $J(V)$ curves was found. Therefore, we conclude that a more refined treatment of final-state effects, and the inclusion of the Coulomb interaction, will not alter the results of the analyses given in this paper.

Figure 3(b) shows the results of a best fit to the $J(V)$ curves for the 122 nm device, based on the mobility model described by Eqs. (3)–(5) and using the drift-diffusion device model presented in Ref. 28. Within the framework of the EGDM, the *shape* of the temperature-dependent $J(V)$ curves, with J plotted on a logarithmic scale and for V_{bi} larger than approximately 0.3 eV, is fully determined by the "primary" model parameters σ and N_t. The "secondary" model parameters ($\mu_{0,\text{EGDM}}$ and V_{bi}) determine only the *position* of the $J(V)$ curve. V_{bi} is treated as a temperature-independent parameter. For each temperature, the remaining free parameter is then $\mu_{0,\text{EGDM}}(T)$. The full curves shown in the figure were obtained using $N_t = 6 \times 10^{26}$ m^{-3} and $\sigma = 0.13$ eV. It is clear

TABLE I. Overview of the model parameter values that optimally describe the experimental $J(V)$ curves. The parameters $\mu_{0,\text{EGDM}}^*$ and C describe the temperature dependence of the mobility in the zero density and zero-field limit and are defined by Eq. (6).

Parameter	Value
σ[eV]	0.13 ± 0.01
N_t[10^{26} m^{-3}]	6 ± 1
V_{bi}[V]	1.95 ± 0.05
ε_r	3.2 ± 0.1
$\mu_{0,\text{EGDM}}^*$[10^{-7} m^2 V^{-1} s^{-1}]	1.4 ± 0.6
C	0.39 ± 0.01

that also the EGDM excellently describes the $J(V)$ curves of the 122 nm device. It is therefore not possible to discriminate between the conventional mobility model and the EGDM on the basis of an analysis of the temperature-dependent $J(V)$ curves for *one single device thickness*.

Figures 5(c) and 5(d) show the experimental $J(V)$ curves for the three thicknesses investigated, for 295 K and 170 K, respectively, as well as the predictions based on the parameter set that has been deduced from the study of the 122 nm devices, discussed above. It is clear that the EGDM, taking the carrier-concentration dependence of the mobility into account, excellently describes the full thickness *and* temperature dependence of the hole transport. This is the first complete drift-diffusion analysis of $J(V)$ curves for an organic electronic device using the carrier concentration and field-dependent mobility that follows from the assumption of a Gaussian DOS.

We have investigated the sensitivity of the quality of the fits in Figs. 3(b), 5(c), and 5(d) to variations of the parameter values using the following procedure: First, the temperature-dependent $J(V)$ curves for the thickest device (122 nm) have been fitted for values of N_t that are a factor of 3 smaller and larger than the optimal value, and for a wide range of σ values. Subsequently, the range of σ values considered is narrowed down by fitting the room temperature $J(V)$ curves of the thickest device, leading to optimized values of $\mu_{0,\text{EGDM}}$ and V_{bi} for the selected $\{N_t, \sigma\}$ combination. For each $\{N_t, \sigma\}$ combination the built-in voltage as determined for the room-temperature data is used for fitting the data at the other temperatures. It is found that a relatively low N_t value leads to a relatively low σ value and gives rise to good fits only at the highest temperatures, whereas a relatively high N_t value leads to a relatively high σ value and gives rise to a good description of the experimental $J(V)$ curves mainly at the lowest temperatures. The best fits were obtained for N_t in the range $(6 \pm 1) \times 10^{26}$ m^{-3}, σ in the range 0.13 ± 0.01 eV, and V_{bi} in the range 1.95 ± 0.05 V. An overview of these results is given in Table I.

The width of the DOS, 0.13 eV, is close to the value obtained for two different PPV derivatives.[24] The value of σ is larger than and approximately equal to the values in the ranges 0.06–0.10 eV and 0.09–0.14 eV, respectively, obtained using various forms of the *conventional* mobility model for the homopolymer poly(9,9-dioctylfluorene) (PFO) (Refs. 7(c) and 39) and for various fluorene-amine copoly-

mers, respectively.[39] We regard the value of σ obtained from our analysis as a true measure of the width of the DOS for the HT units, as we have found from a study of the HT-unit concentration dependence of the current density that the transport is well in the guest-to-guest hopping regime.[34] We have thus no indication that σ is an effective width of the cumulative host plus guest DOS. This point of view is consistent with the large ($\sim$0.6 eV) distance between the host and guest HOMO energies, and the relatively small width of the DOS of the PF homopolymer, obtained in the literature [Refs. 7(c) and 39].

The optimal value of the built-in voltage, 1.95 V, is approximately 0.3 V larger than found for the conventional mobility model. The difference may be understood as a result of the fact that transport in a Gaussian DOS occurs by hopping in between states which are situated a few tenths of an eV below the top of the DOS. The effective onset voltage, at which the current density shows a steep increase with the voltage, decreases therefore with increasing σ, as demonstrated quantitatively in Ref. 28. Preliminary modeling of the capacitance-voltage curves, within the framework of the EGDM and using the material parameters given in Table I, leads to a value of V_{bi} that is consistent with the value given in the table.[45]

For the thinner devices, the conventional model underestimates the current density at high voltages and at low temperatures, if the model parameters are obtained from an analysis for the thickest device (Sec. III A). The EGDM provides a much better description to the $J(V)$ curves, for all thicknesses and temperatures. This can be understood from the carrier-concentration dependence of the mobility. In a thin device, the hole concentration at a given voltage is at any relative position x/L larger than in a thick device. As the mobility increases with carrier concentration, the (average) mobility is larger for a thin device, which leads to a larger current density. Furthermore, a lowering of the temperature leads to a larger value of $\sigma/(k_B T)$, enhancing the carrier-concentration dependence of the mobility [see Eq. (3) and Ref. 24]. Therefore, the deviations between experiment and the predictions made from the conventional model are even larger at low temperatures. For a systematic analysis of this effect, we refer to Ref. 28.

Figure 6 shows the temperature dependence of $\mu_{0,\text{EGDM}}$, the mobility in the low carrier density and low electric-field limit, which is predicted to be of the form[25]

$$\mu_{0,\text{EGDM}}(T) = \mu^*_{0,\text{EGDM}} \exp\left[-C\left(\frac{\sigma}{k_B T}\right)^2\right]. \quad (6)$$

Here, C is a dimensionless parameter which depends on the wave-function decay length. The figure shows that the temperature dependence of $\mu_{0,\text{EGDM}}$ is excellently described by Eq. (6), with $C=0.39$. This value falls well in the range of $C=0.38$ to 0.46, expected for disordered organic semiconductors.[25] Making use of the dependence of C on the wave-function decay length obtained in Ref. 25, we estimate that it is slightly larger than $0.1 \times a$, with (from Table I) $a = N_t^{-1/3} = 1.2$ nm.
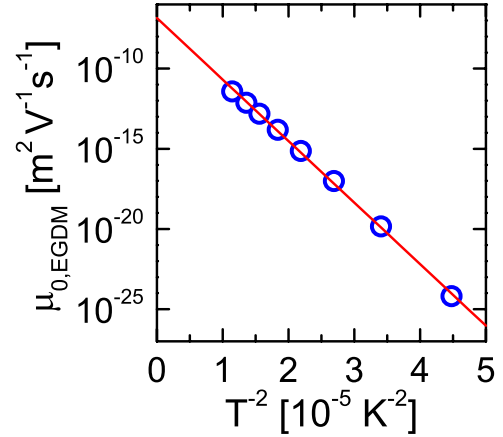

FIG. 6. (Color online) Temperature dependence of $\mu_{0,\text{EGDM}}$, the mobility in the Boltzmann limit and at zero field (solid circles), obtained from the analysis described in Sec. III B. The full curve gives a fit using Eq. (6) with $C=0.39$.

IV. $1/T$ VERSUS $1/T^2$ DEPENDENCE OF THE MOBILITY

In Sec. III B it was demonstrated that the EGDM leads to an excellent description of the hole transport. In this section we discuss how it can be understood that many mobility studies on organic semiconductor devices show a $1/T$ temperature dependence of the logarithm of the mobility, while other studies, including the present study using the EGDM, predict a $1/T^2$ dependence, as demonstrated in Fig. 6. We show that this paradoxical situation can be understood within the framework of the EGDM, and we compare the temperature dependence of the mobility as predicted from the EGDM with the results obtained for various other organic semiconductors by Craciun $et\ al.$,[35] as discussed in Sec. I.

A commonly used approach to determine 'the' mobility is by applying the MG square law [Eq. (2)] to measured $J(V)$ curves, after the application of a built-in voltage correction. An example of such an analysis is shown in the inset of Fig. 2. The squares in Fig. 7 show the result of this approach, applied to the experimental $J(V)$ curves for the 122 nm devices, shown in Fig. 3. It is clear that this leads to an apparent $1/T$ dependence of the mobility. In fact, the determined mobility is an $effective$ mobility (μ_{eff}) for this 122 nm device, containing a finite carrier density. It is not equal to the mobility in the low carrier density Boltzmann regime (and for a low electric field), $\mu_{0,\text{EGDM}}(T)$, given by Eq. (6) and indicated in Fig. 7 by a full curve. At room temperature, the difference is already slightly more than a factor of 10.

In principle, it would be possible to directly determine $\mu_{0,\text{EGDM}}$ using the MG square-law approach by making use of a very thick device, as the charge carrier concentration and the electric field are then very low in a very large part of the device. Furthermore, the role of diffusion is then reduced and small errors in the determination of the built-in voltage play a less important role than for the case of a thin device. Recently, Craciun $et\ al.$[29] showed that the effective hole mobility in 40 to 320 nm MEH-PPV-based devices, as obtained from the $J(V)$ curves in a manner as described above, indeed increases with decreasing thickness. Using a phenomenological model for the carrier-concentration dependence of the
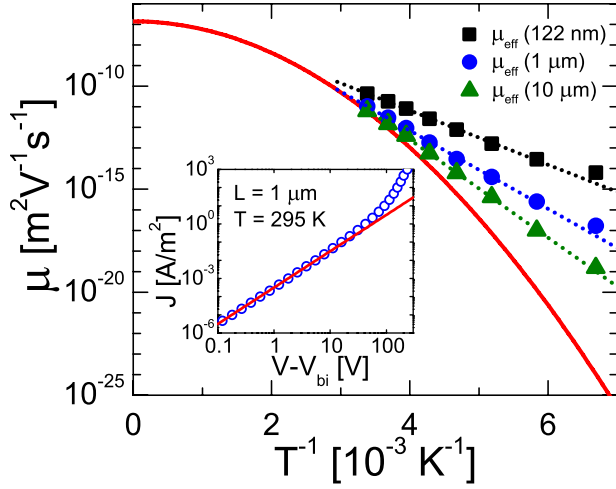
FIG. 7. (Color online) Comparison of the effective mobility $[\mu_{\mathrm{eff}}(T)]$ for 122 nm, 1 μm and 10 μm devices with the function $\mu_{0,\mathrm{EGDM}},(T)$ (full curve). The method for determining μ_{eff} is described in Sec. IV. The inset shows the calculated $J(V)$ curve for a 1 μm device at 295 K. The line is a fit of the data for $V<10$ V using Eq. (2).

mobility, the effective mobility at room temperature was argued to be enhanced by a factor of 2.5 as compared to the mobility in the low-carrier density limit. For the blue-emitting polyfluorene-based polymer investigated in this paper, we have obtained a qualitatively similar result. In order to investigate this issue more quantitatively, within the EGDM, we have calculated the temperature-dependent effective mobilities for 1- and 10 μm-thick devices (circles and triangles, respectively, in Fig. 7), using the model parameters given in Table I. The inset in the figure shows how, for the case of a 1 μm device at 295 K, the effective mobility is determined using the MG square-law approach from the $J(V)$ curve. It is clear from Fig. 7 that also for these thicker devices, an approximate $1/T$ temperature dependence is obtained within a rather large temperature range below room temperature. For all temperatures used, the effective mobility decreases with increasing device thickness. However, even for a 10 μm-thick device $\mu_{\mathrm{eff}}(T)$ is still significantly larger than $\mu_{0,\mathrm{EGDM}}(T)$ throughout the entire temperature range studied. At room temperature, μ_{eff} is approximately 2 $\times \mu_{0,\mathrm{EGDM}}$. We thus conclude that only for thicknesses that are unrealistically large for OLEDs, the MG approach could be used to obtain the mobility in the low carrier density and low electric-field limit. For more realistic thicknesses, in the order of 100 nm, a full analysis of the temperature and thickness-dependent $J(V)$ curve is needed using the EGDM.

These results are fully consistent with the theoretical predictions from Coehoorn *et al.*[25] for transport in a Gaussian DOS, viz. that for carrier concentrations above a crossover value c^* (see Sec. III B) the logarithm of the mobility shows an effective $1/T$ temperature dependence for a rather broad temperature range. For the polyfluorene-based material studied in this paper, $c^*=1.5\times10^{-6}$ at room temperature. It is striking, though, that this does not only hold for the temperature dependence of the mobility at a *specific* carrier concentration, as in Ref. 25, but apparently also for the effective

mobility of a *complete device* in which the carrier concentration depends strongly on the position x in the device. This explains why commonly used methods to determine the mobility, such as dark-injection transient measurements, steady-state $J(V)$ measurements, admittance spectroscopy measurements, and even time-of-flight measurements on relatively thick samples, often lead to an apparent $1/T$ temperature dependence of the mobility, even when there is clear evidence of the predominant role of disorder.

As discussed already in Sec. I, a $1/T$ dependence of the mobility has often been observed, which has been viewed as an indication that the activation energy for the hopping transport is related to the energy associated with polaron formation. We argue, however, that the finding of a $1/T$ dependence can be well explained by taking energetic disorder into account, as described by a Gaussian DOS. For the material studied here, the mobility can be only consistently modeled assuming a predominant role of the energetic disorder, as demonstrated in Sec. III. This indicates that the effective activation energy related to the disorder, $E_{A,\mathrm{disorder}}$, is large as compared to the activation energy associated with polaron hopping, $E_{A,\mathrm{pol}}$. Following Bässler[46] and Fishchuk,[47] the total effective Arrhenius activation energy for charge carrier hopping may be written as $E_{A,\mathrm{tot}}=E_{A,\mathrm{pol}}+E_{A,\mathrm{disorder}}=E_{\mathrm{pol},b}/2+2C\times\sigma^2/(k_BT)$. Here, $E_{\mathrm{pol},b}$ is the polaron binding energy, and C is a dimensionless number as defined (within the EGDM) in Eq. (6). For the material studied in this paper, $E_{A,\mathrm{disorder}}\approx0.52$ eV at room temperature. Our analysis thus implies that $E_{A,\mathrm{pol}}$ is much smaller than 0.5 eV. In this sense, the situation is similar as in PPV, for which $\sigma\approx0.14$ eV (Ref. 24) so that $E_{A,\mathrm{disorder}}\approx0.5-0.6$ eV, whereas $E_{A,\mathrm{pol}}$ is much smaller than 0.05 eV (using the theoretical value $E_{\mathrm{pol},b}\leq0.05$ eV found by Meisel *et al.*[48]).

Figure 7 shows that the $1/T$ dependence of $\log(\mu_{\mathrm{eff}})$ breaks down at low temperatures, i.e., below approximately 170 K for the system studied. Also this finding is consistent with the predictions given by Coehoorn *et al.* in Ref. 25. We regard this change of slope as a result of a gradual transition from the nearest-neighbor hopping regime to the variable-range hopping regime at low temperatures.

In conclusion, it is predicted from the EGDM that over a large temperature range the effective mobility shows (i) a $1/T$ dependence, (ii) is layer thickness dependent, and (iii) extrapolates to a $1/T^2$ dependence for sufficiently large thicknesses. The EGDM, within which all our temperature and layer thickness dependent results can be consistently described, does *not* predict that the effective mobility would extrapolate to a layer thickness independent universal value for $1/T\to0$, as was suggested by Craciun *et al.*[35]

V. SUMMARY AND CONCLUSIONS

We find that the current-voltage curves of hole-only devices containing a blue-emitting polyfluorene-based copolymer can be consistently described, for a wide range of temperatures and layer thicknesses, using a drift-diffusion device model within which the mobility is described using the extended Gaussian disorder model. Within a conventional model, which neglects the carrier-concentration dependence

of the mobility and which treats the field dependence using a Poole-Frenkel factor, good descriptions of the $J(V)$ curves can be obtained for a single layer thickness, but not simultaneously for all thicknesses studied. We note that this conventional approach has been proposed in many earlier studies. See, for example, Refs. 8, 12, 14–18, 39, and 42. The model parameters as obtained using the EGDM, summarized in Table I, have realistic values. The width of the DOS, σ =0.13 eV, is in the range of values found previously for disordered organic semiconductors.[10,12,14,24,39,49] The site density obtained, $N_t = 6 \times 10^{26}$ m^{-3}, may be compared with the estimated volume density of copolymerized hole transporting units, $\sim 1.8 \times 10^{26}$ m^{-3}.[34] The analysis is supported by the observation that a $1/T^2$ temperature dependence of the mobility in the low carrier density and field limit has been found of the form $\mu_{0,EGDM} \propto \exp(-C\hat{\sigma}^2)$, with $C=0.39$, which is consistent with theoretical predictions given in Ref. 25.

We have shown that analyses of the $J(V)$ curves using (incorrectly) a Mott-Gurney square-law approach lead to effective mobilities which (on a log scale) vary with temperature as $1/T$, and that these mobilities are layer thickness dependent. Only for unrealistically large thicknesses, of 10 μm or larger (depending on the temperature), the mobility as obtained in this way is close to $\mu_{0,EGDM}$. Due to this layer thickness dependence, the values of μ_{eff}, as obtained from a study for one layer thickness, are not a proper basis for the modeling of OLEDs. Our study thus shows that the often-found $1/T$ dependence of μ_{eff} can be explained within the EGDM, whereas the more fundamental mobility parameter $\mu_{0,EGDM}$ varies as $1/T^2$. We believe that our work thereby contributes to solving the long-standing controversy concerning the temperature dependence of the mobility.

*siebe.van.mensfoort@philips.com

[1] S. R. Forrest, Nature (London) **428**, 911 (2004).

[2] E. I. Haskal, M. Büchel, P. C. Duineveld, A. Stempel, and P. van de Weijer, MRS Bull. **27**, 864 (2002).

[3] B. W. D'Andrade and S. R. Forrest, Adv. Mater. (Weinheim, Ger.) **16**, 1585 (2004).

[4] G. G. Malliaras and J. C. Scott, J. Appl. Phys. **83**, 5399 (1998).

[5] M.-H. Lu and J. C. Sturm, J. Appl. Phys. **91**, 595 (2002).

[6] B. Ruhstaller, S. A. Carter, S. Barth, H. Riel, W. Riess, and J. C. Scott, J. Appl. Phys. **89**, 4575 (2001).

[7] (a) L. B. Schein, D. Glatz, and J. C. Scott, Phys. Rev. Lett. **65**, 472 (1990); (b) L. Th. Pautmeier, J. C. Scott, and L. B. Schein, Chem. Phys. Lett. **197**, 568 (1992); (c) T. Kreouzis, D. Poplavskyy, S. M. Tuladhar, M. Campoy-Quiles, J. Nelson, A. J. Campbell, and D. D. C. Bradley, Phys. Rev. B **73**, 235201 (2006).

[8] H. Bässler, Phys. Status Solidi B **175**, 15 (1993).

[9] V. I. Arkhipov, P. Heremans, E. V. Emelianova, G. J. Adriaenssens, and H. Bässler, J. Phys.: Condens. Matter **14**, 9899 (2002).

[10] P. M. Borsenberger, W. T. Gruenbaum, U. Wolf, and H. Bässler, Chem. Phys. **234**, 277 (1998); P. M. Borsenberger and D. S. Weiss, *Organic Photoreceptors for Xerography* (Dekker, New York, 1998).

[11] D. Poplavskyy, W. Su, and F. So, J. Appl. Phys. **98**, 014501 (2005).

[12] P. W. M. Blom and M. C. J. M. Vissenberg, Mater. Sci. Eng., R. **27**, 53 (2000).

[13] J. Staudigel, M. Stössel, F. Steuber, and J. Simmerer, Appl. Phys. Lett. **75**, 217 (1999).

[14] S. Doi, T. Yamada, Y. Tsubata, and M. Ueda, Proc. SPIE **5519**, 161 (2004).

[15] D. M. Pai, J. F. Yanus, and M. Stolka, J. Phys. Chem. **88**, 4714 (1984).

[16] J. G. Simmons, Phys. Rev. **155**, 657 (1967).

[17] W. D. Gill, J. Appl. Phys. **43**, 5033 (1972).

[18] S. V. Novikov, D. H. Dunlap, V. M. Kenkre, P. E. Parris, and A. V. Vannikov, Phys. Rev. Lett. **81**, 4472 (1998).

[19] D. Monroe, Phys. Rev. Lett. **54**, 146 (1985).

[20] M. C. J. M. Vissenberg and M. Matters, Phys. Rev. B **57**, 12964 (1998).

[21] B. Maennig, M. Pfeiffer, A. Nollau, X. Zhou, K. Leo, and P. Simon, Phys. Rev. B **64**, 195208 (2001).

[22] R. Schmechel, Phys. Rev. B **66**, 235206 (2002).

[23] C. Tanase, E. J. Meijer, P. W. M. Blom, and D. M. de Leeuw, Phys. Rev. Lett. **91**, 216601 (2003); C. Tanase, P. W. M. Blom, and D. M. de Leeuw, Phys. Rev. B **70**, 193202 (2004).

[24] W. F. Pasveer, J. Cottaar, C. Tanase, R. Coehoorn, P. A. Bobbert, P. W. M. Blom, D. M. de Leeuw, and M. A. J. Michels, Phys. Rev. Lett. **94**, 206601 (2005).

[25] R. Coehoorn, W. F. Pasveer, P. A. Bobbert, and M. A. J. Michels, Phys. Rev. B **72**, 155206 (2005).

[26] I. I. Fishchuk, V. I. Arkhipov, A. Kadashchuk, P. Heremans, and H. Bässler, Phys. Rev. B **76**, 045210 (2007).

[27] Y. Roichman, Y. Preezant, and N. Tessler, Phys. Status Solidi A **201**, 1246 (2004).

[28] S. L. M. van Mensfoort and R. Coehoorn, preceding paper, Phys. Rev. B **78**, 085207 (2008).

[29] N. I. Craciun, J. J. Brondijk, and P. W. M. Blom, Phys. Rev. B **77**, 035206 (2008).

[30] H. H. Fong, A. Papadimitratos, and G. G. Malliaras, Appl. Phys. Lett. **89**, 172116 (2006).

[31] W. Wu, M. Inbasekaran, M. Hudack, D. Welsh, W. Yu, Y. Cheng,

C. Wang, S. Kram, M. Tacey, M. Bernius, R. Fletcher, K. Kiszka, S. Munger, and J. O'Brien, Microelectron. J. **35**, 343 (2004).

[32] N. C. van der Vaart, H. Lifka, F. P. M. Budzelaar, J. E. J. M. Rubingh, J. J. L. Hoppenbrouwers, J. F. Dijksman, R. G. F. A. Verbeek, R. van Woudenberg, F. J. Vossen, M. G. H. Hiddink, J. W. M. Rosink, T. N. M. Bernards, A. Giraldo, N. D. Young, D. A. Fish, M. J. Childs, W. A. Steer, D. Lee, and D. S. George, J. Soc. Inf. Disp. **13**, 9 (2005).

[33] P. W. M. Blom, C. Tanase, D. M. de Leeuw, and R. Coehoorn, Appl. Phys. Lett. **86**, 092105 (2005).

[34] R. Coehoorn, S. I. E. Vulto, S. L. M. van Mensfoort, J. Billen, M. Bartyzel, H. Greiner, and R. Assent, Proc. SPIE **6192**, 61920O (2006).

[35] N. I. Craciun, J. Wildeman, and P. W. M. Blom, Phys. Rev. Lett. **100**, 056601 (2008).

[36] Baytron® P AI4083, obtained from H. C. Starck.

[37] A. Kahn, N. Koch, and W. Gao, J. Polym. Sci., Part B: Polym. Phys. **41**, 2529 (2003); C. Tengstedt, W. Osikowicz, W. Salaneck, I. D. Parker, C.-H. Hsu, and M. Fahlman, Appl. Phys. Lett. **88**, 053502 (2006).

[38] P. Stallinga, H. L. Gomes, H. Rost, A. B. Holmes, M. G. Harrison, and R. H. Friend, J. Appl. Phys. **89**, 1713 (2001).

[39] R. U. A. Khan, D. Poplavskyy, T. Kreouzis, and D. D. C. Bradley, Phys. Rev. B **75**, 035215 (2007).

[40] M. A. Lampert and P. Mark, *Current Injection in Solids* (Academic, New York, 1970).

[41] S. L. M. van Mensfoort and R. Coehoorn, Phys. Rev. Lett. **100**, 086802 (2008).

[42] W. Brütting, S. Berleb, and A. G. Mückl, Synth. Met. **122**, 99 (2001); A. K. Kapoor, S. C. Jain, J. Poortmans, V. Kumar, and R. Mertens, J. Appl. Phys. **92**, 3835 (2002); S. F. Singh and V. L. Gupta, Electron. Lett. **39**, 862 (2003).

[43] Y. Roichman and N. Tessler, Appl. Phys. Lett. **80**, 1948 (2002).

[44] J. Zhou, Y. C. Zhou, J. M. Zhao, C. Q. Wu, X. M. Ding, and X. Y. Hou, Phys. Rev. B **75**, 153201 (2007).

[45] S. L. M. van Mensfoort, W. C. Germs, and R. Coehoorn (unpublished).

[46] H. Bässler, P. M. Borsenberger, and R. J. Perry, J. Polym. Sci., Part B: Polym. Phys. **32**, 1677 (1994).

[47] I. I. Fishchuk, A. Kadashchuk, H. Bässler, and S. Nešpůrek, Phys. Rev. B **67**, 224303 (2003).

[48] K. D. Meisel, H. Vocks, and P. A. Bobbert, Phys. Rev. B **71**, 205206 (2005).

[49] T. N. Ng, W. R. Silveira, and J. A. Marohn, Phys. Rev. Lett. **98**, 066101 (2007).